Smart Structures and Systems, *Vol. 22, No. 4 (2018) 399-411*
DOI: https://doi.org/10.12989/sss.2018.22.4.399

Uncertainty quantification for structural health monitoring applications

Dana E. Nasr[a], Wael G. Slika[b] and George A. Saad[*]

Department of Civil and Environmental Engineering, American University of Beirut, Beirut, Lebanon

(Received November 13, 2017, Revised September 1, 2018, Accepted September 3, 2018)

Abstract. The difficulty in modeling complex nonlinear structures lies in the presence of significant sources of uncertainties mainly attributed to sudden changes in the structure's behavior caused by regular aging factors or extreme events. Quantifying these uncertainties and accurately representing them within the complex mathematical framework of Structural Health Monitoring (SHM) are significantly essential for system identification and damage detection purposes. This study highlights the importance of uncertainty quantification in SHM frameworks, and presents a comparative analysis between intrusive and non-intrusive techniques in quantifying uncertainties for SHM purposes through two different variations of the Kalman Filter (KF) method, the Ensemble Kalman filter (EnKF) and the Polynomial Chaos Kalman Filter (PCKF). The comparative analysis is based on a numerical example that consists of a four degrees-of-freedom (DOF) system, comprising Bouc-Wen hysteretic behavior and subjected to El-Centro earthquake excitation. The comparison is based on the ability of each technique to quantify the different sources of uncertainty for SHM purposes and to accurately approximate the system state and parameters when compared to the true state with the least computational burden. While the results show that both filters are able to locate the damage in space and time and to accurately estimate the system responses and unknown parameters, the computational cost of PCKF is shown to be less than that of EnKF for a similar level of numerical accuracy.

Keywords: system identification; uncertainty quantification; sequential data assimilation; ensemble Kalman filter; polynomial chaos Kalman filter

1. Introduction

Building structures commonly exhibit non-linear dynamical behavior with uncertain and complex governing laws. Accurate mathematical representation of such systems is essential for system identification and damage detection purposes. The Bouc-Wen hysteretic model is extensively used in the literature to simulate the complex non-linear dynamics of structural elements. The Bouc-Wen model, consisting of a first order nonlinear differential equation, relates the input displacement to the output restoring force that is function of not only the input but also incorporates some history dependence. Hassani *et al.* and Ismail *et al.* presented review works and surveys in hysteresis modeling and identification, especially concerning the hysteretic Bouc-Wen model (Ismail *et al.* 2009, Hassani *et al.* 2014). On the other hand, many authors, such as Song and Der Kiureghian 2006, Ye and Wang 2007, Ikhouane *et al.* 2007, Zhang *et al.* (2002), studied the model parameters, mainly for parameters $(\alpha, \beta, \gamma, n\ and\ A)$, and the dynamic properties of the Bouc-Wen hysteretic model (Zhang *et al.* 2002, Song and Der Kiureghian 2006, Ikhouane *et al.* 2007, Ye and Wang 2007). As parameter α represents the ratio of linear to nonlinear response of the system, parameter n, on the other side, governs the smoothness of the transition from the linear to the nonlinear range. Parameters $\beta\ and\ \gamma$ influence the hardening and softening behavior of the system. These two previously mentioned parameters, along with parameter A, control the general shape and size of the hysteresis loop. The challenge lies in developing robust system identification techniques that can be used for characterizing such mathematical model parameters for SHM and damage detection purposes.

With the recent developments in monitoring technologies such as high performance sensors, optical or wireless networks, and the global position system, SHM measurement data became very abundant which leads to the problem of dealing with the large flow of data (Doebling *et al.* 1996, Sohn *et al.* 2002, Chang *et al.* 2003, Farrar and Worden 2007, Goyal and Pabla 2015). Data assimilation (DA) techniques are commonly adopted to characterize the state and parameters of unknown systems using observed measurements. They were first developed for weather forecasting and ocean state estimation (Daley 1997, Kalnay 2003), then started to be used for many other applications including the system identification and SHM fields. The DA techniques are classified into two main categories: variational data assimilation and sequential data assimilation. The first class aims at minimizing a certain cost function that describes the misfit between the model and actual data to find a solution to a numerical forecast model, using gradient-based optimization and adjoint methods (LeDimet and Talagrand 1986, Navon e*t al.* 1992). The main drawback of this class of data assimilation methods is that it is computationally expensive. Whereas

∗Corresponding author, Associate Professor
E-mail: george.saad@aub.edu.lb
[a] Ph.D. Candidate
E-mail: den01@mail.aub.edu
[b] Ph.D. Candidate
E-mail: wgs02@mail.aub.edu

http://www.techno-press.com/journals/sss&subpage=7 ISSN: 1738-1584 (Print), 1738-1991 (Online)

the second class, Sequential Data Assimilation, is based on predicting information forward in time to estimate the state of the system using its probabilistic framework and therefore overcoming the need to derive an inverse model and saving computational burden (Evensen 1994, Bertino *et al.* 2003).

The sequential data assimilation techniques consist mainly of the Bayesian probabilistic approach and the Kalman filter technique with its different variations. The Kalman filter is an optimal recursive Bayesian filter for the case of linear dynamical systems with Gaussian errors. Extensions of the original KF to the extended Kalman filter (EKF) based on some linearization techniques are suggested in the literature to handle more general cases (Chui and Chen 1991, Corigliano and Mariani 2004). For highly nonlinear models and for models subjected to significant non-Gaussian noise, the EKF does not provide consistent estimations of the state and model parameters (Lei *et al*. 2015, Xu and He 2015). Other variations of the standard KF were suggested in the literature to overcome the major drawbacks of the EKF. Some of the nonlinear extensions of the standard KF are based on sampling techniques, such as the unscented KF (Kandepu *et al.* 2008, Chatzi and Fuggini 2015, Liu *et al*. 2015, Al-Hussein and Haldar 2016), the particle filter (Chatzi and Smyth 2009, Chatzi and Smyth 2013), the cubature filter (Arasaratnam and Haykin 2009) and the ensemble Kalman filter (Ghanem and Ferro 2006, Evensen 2009, Slika and Saad 2016) and others are based on non-sampling techniques, such as the polynomial chaos Kalman filter (Saad and Ghanem 2009, Saad and Ghanem 2011, Slika and Saad 2016, Slika and Saad 2017). Due to their computational efficiency, the sequential data assimilation techniques are more commonly adopted in the literature for damage detection and system identification problems than the variational data assimilation methods.

Many researchers have investigated the use of sequential data assimilation techniques for SHM purposes in a number of publications in the past years. A number of works presenting a comparison between the UKF and EKF techniques in estimating the system state and parameters are available in the literature (St-Pierre and Gingras 2004, Kandepu *et al.* 2008, Chowdhary and Jategaonkar 2010). In these works, the UKF required higher computational burden while maintaining comparable or slightly better performance than the EKF in terms of robustness and accuracy. Chatzi and Smyth compared the UKF to two different particle filter (PF) techniques, the generic PF and the Gaussian mixture sigma point particle filter (GMSPPF), based on the computational expediency and the efficiency in estimating the state and parameters of nonlinear complex systems using the Bouc-Wen model (Chatzi and Smyth 2009). While the UKF was found to be the most computationally efficient method, the GMSPPF was the most accurate and robust technique in estimating the model parameters. These aforementioned authors then proposed a novel method, the mutated PF (MPF), for nonlinear, non-Gaussian online state and Bouc-Wen parameter estimations for SHM purposes (Chatzi and Smyth 2013). The proposed algorithm outperformed the standard PF and the UKF in both computational cost and accuracy.

Hommels *et al*. (2009), applied the EnKF and the UKF on a conceptual nonlinear case study based on the construction of a road embankment (Hommels *et al*. 2009). While both methods needed the same computational time, the EnKF outperformed the UKF. Ghanem and Ferro proved that the EnKF plays a role of a good estimator of the system state (Ghanem and Ferro 2006). In their work, they combined the EnKF with a non-parametric modeling technique and compared it to the EKF method to show the benefits of their method. Evensen (2009) presented a detailed literature review on the applications of the EnKF as a sequential Monte Carlo (MC) method and concentrated on its use for state and parameter estimation through a number of numerical examples. Slika and Saad developed a robust non-destructive EnKF based SHM framework for assessing the health conditions of a structure and predicting its remaining service life without corrosion using a finite element/finite difference scheme (Slika and Saad 2016).

In case of highly nonlinear systems, the EnKF requires a large number of ensembles to properly approximate the model state statistics. To solve this problem, the Polynomial Chaos Kalman Filter (PCKF) was introduced by Saad and Ghanem (Saad 2007, Saad and Ghanem 2009, Saad and Ghanem 2011). Polynomial chaos decompositions of the uncertain parameters are propagated forward in time using the Galerkin projection approach, then updated every time measurements are recorded (Ghanem 1999, Ghanem and Spanos 2003). Li and Xiu (Li and Xiu 2009) presented a variation of the PCKF where he proposed to use a set of EnKF algorithms based on generalized polynomial chaos (gPC) expansion. The method is a two-step approach; two different routines can be used to solve the system of state equations in the first step (forecast step), the stochastic Galerkin and the stochastic Collocation approaches. The gPC expansion is then applied to generate arbitrarily large ensemble of realizations to find the state estimates in the second step (analysis step) for both approaches. Spiridonakos *et al* (2016) suggested a new method, based on combining the polynomial chaos expansion (PCE) method with the independent component analysis (ICA) algorithm, to monitor the health conditions of structures subjected to operational variability (Spiridonakos *et al.* 2016).

The main challenge associated with the aforementioned existing sequential data assimilation methods is the presence of different forms of uncertainties due to many sources of errors when dealing with complex and nonlinear systems. These errors are magnified due to regular aging factors and deterioration of the structure or due to some extreme events, such as earthquakes, that could alter its behavior unexpectedly.

This study highlights the importance of uncertainty quantification in SHM frameworks, and presents a comparative analysis between intrusive and non-intrusive techniques in quantifying uncertainties for SHM purposes through two different variations of the Kalman Filter (KF) method, the Ensemble Kalman filter (EnKF) and the Polynomial Chaos Kalman Filter (PCKF)

These two approaches are applied on a four-degrees-of-freedom system subjected to El-Centro earthquake excitation. All DOFs are assumed to undergo degrading hysteretic behaviors described by the Bouc-Wen model. A predefined damage of the first DOF is imposed ten seconds after the excitation hits the system. The comparison is based on the ability of each method in quantifying the uncertainty for SHM purposes with the least computational burden and leading to the most accurate results.

The paper is divided into five sections. The second section represents the mathematical formulations of the different sequential data assimilation techniques used. The third section consists of a numerical problem composed of a four-DOF system subjected to seismic excitation and used to compare the EnKF with the PCKF methods in quantifying the uncertainty. The results of the numerical problem are exposed and discussed in the fourth section. Finally, general conclusions are drawn in section five.

2. Mathematical formulations of sequential data assimilation techniques

The Kalman Filter (KF) (Kalman 1960, Burgers *et al.* 1998, Welch and Bishop 2006, Grewal and Andrews 2008) is an optimal recursive data processing estimator that approximates the state of linear dynamical systems perturbed by Gaussian white noise, using observations that are subjected to Gaussian errors. This process involves two stages, the first stage is the forecast or predictive stage, where the model state at time k is propagated forward in time, and the second stage is the update or corrective stage, where the variables describing the state of the system are adjusted based on the actual measurements at time k+1.

2.1 Ensemble Kalman Filter

For the case of nonlinear systems or systems subjected to non-Gaussian errors, many variations of the Kalman Filter can be used. One of the most widely used approximate techniques is the EKF that was first introduced by Chui and Chen (Chui and Chen 1991) and clearly discussed in (Welch and Bishop 2006); it is based on some linearization processes. But this variation of the KF showed some drawbacks, especially regarding its high computational cost and its difficulty to be a good estimator in the case of highly nonlinear systems and significant non-Gaussian noise. The EnKF was introduced by Evensen (Evensen 1994) to overcome some of the limitations of the standard KF and the EKF, and then improved and developed in many works (Burgers *et al*. 1998, Evensen 2003, Gillijns *et al.* 2006, Welch and Bishop 2006, Evensen 2009). The EnKF is a non-intrusive technique based on Monte Carlo sampling; it propagates an ensemble of realizations forward in time and solves the forward problem under consideration using a black-box model, then corrects the propagated system states and parameters whenever measurements are available.

The EnKF consists of first evaluating the ensemble matrix A, holding the ensemble members xi

$$A = (x_1, x_2, \dots, x_N) \quad A \in R^{n\times N}, x_i \in R^n \tag{1}$$

where n is the size of the model state vector and N is the number of ensemble members.

The ensemble mean and ensemble perturbation matrices are respectively evaluated as follows

$$\bar{A} = A1_N \; \bar{A} \in R^{n\times N} \tag{2}$$

$$A' = A - \bar{A} = A(I - 1_N) \quad A' \in R^{n\times N} \tag{3}$$

where $1_N \in R^{N\times N}$ is a matrix having its elements equal to 1/N.

The ensemble covariance matrix is next calculated as

$$P = \frac{1}{N-1} A' A'^T \quad P \in R^{n\times n} \tag{4}$$

The analysis equation is the following

$$A^a = A^f + KG(D - HA^f) \tag{5}$$

where KG is the same Kalman Gain used in the standard KF

$$KG = P^f H^T (HP^f H^T + R)^{-1} \tag{6}$$

D is the ensemble of observation matrix holding the measurement vectors $d \in R^m$

$$D = (d_1, d_2, \dots, d_N) \quad D \in R^{m\times N} \tag{7}$$

where m is the number of measurements, and

$$d_j = d + \epsilon_j \quad j = 1, \dots, N \tag{8}$$

where ϵ_j is the measurement noise vector.
H is the measurement operator connecting the true state to the observations and R is the measurement error covariance matrix defined by

$$R = \frac{1}{N-1} \gamma\gamma^T \quad R \in R^{m\times m} \tag{9}$$

where γ is the ensemble of perturbations expressed as

$$\gamma = (\epsilon_1, \epsilon_2, \dots, \epsilon_N) \quad \gamma \in R^{m\times N} \tag{10}$$

2.2 Polynomial chaos Kalman Filter

Although the EnKF solves the major limitations of the standard KF and the EKF, it still faces some challenges, especially in accurately approximating the model state and parameters of the system when a small ensemble size is used. Furthermore, for highly nonlinear problems, the EnKF requires a large ensemble size which increases the computational cost, that’s why the PCKF was proposed to be used instead (Saad 2007, Saad and Ghanem 2009, Saad and Ghanem 2011). Before going through the details of the PCKF, a brief overview of the Polynomial Chaos Expansion (PCE) (Ghanem and Spanos 2003) is presented next.

Wiener (1938) was the first one to introduce the Polynomial chaos theory in the form of Homogeneous Chaos Expansion that uses Hermite polynomials to model stochastic processes with Gaussian random variables. Every source of uncertainty in the system under consideration is independently represented by a vector of random variables $\xi(\theta)$. All these independent random variables are then correlated with an individual random event θ. Therefore, for each specific problem, the researcher has to determine the size of the vector holding the random variables based on the available sources of uncertainty. A multidimensional orthogonal basis is formed through the expansion of the nonlinear functionals of an appropriate set of ξ. Hence, this multidimensional orthogonal basis is considered as Hermite polynomial in case the random variable under consideration is Gaussian (Saad *et al*. 2007).

Any random process $u(x,\theta)$ with prescribed probability density function, can be expanded as a polynomial function of Multi-dimensional Hermite polynomials in Gaussian random variables (Ghanem and Spanos 2003), as

$$u(x,\theta) = \sum_{i=0}^{\infty} u_i(x)\psi_i\big(\xi(\theta)\big) \tag{11}$$

where $\{u_i, i = 0, \ldots, \infty\}$ are deterministic expansion coefficients that can be evaluated using different methods (Projection Method, Collocation Method,…), $\psi_n(\xi_{i1}, \ldots, \xi_{in})$ is the nth order Polynomial Chaos in the Gaussian variables $(\xi_{i1}, \ldots, \xi_{in})$ and $\{\psi_i, i = 0, \ldots, \infty\}$ are the orthogonal multidimensional Hermite polynomials.
After truncating the polynomial chaos expansion at the Pth term, the above relation becomes

$$u(x,\theta) = \sum_{i=0}^{P} u_i(x)\psi_i\big(\xi(\theta)\big) \tag{12}$$

where P+1 is the total number of terms in a polynomial chaos expansion. For an order less than or equal to p and a dimension equals to M, P+1 is equal to

$$P + 1 = \frac{(p+M)!}{p!\,M!} \tag{13}$$

The PCKF is a sampling-free intrusive sequential data assimilation method based on representing the system state and parameters by their corresponding polynomial chaos representations (Saad 2007, Saad and Ghanem 2009). Instead of propagating an ensemble of realizations forward in time, as in the case of the EnKF, the PCKF allows the propagation of the PC representations of the unknown variables. This intrusive technique requires the user to go through the black-box model and modify the equation of motions to account for these PC decompositions, which makes it a more complicated method than the ordinary EnKF approach.
In the PCKF (Saad 2007, Saad and Ghanem 2009), the forecast step is based on propagating the state vector forward in time and applying the Galerkin projection method to solve the system.
The matrix holding the chaos coefficients is represented as follow

$$A = (x_0, x_1, \ldots, x_P) \quad A \in R^{n\times(P+1)} \tag{14}$$

where x_0 is the mean of the model state x, stored in the first column of A, $\{x_1, \ldots, x_P\}$ are the model state perturbations, stored in the remaining columns of A, P+1 is the total number of terms in the polynomial chaos representation of the model state, n is the size of the model state vector x that is represented as

$$x = \sum_{i=0}^{P} x_i(x)\psi_i\big(\xi(\theta)\big) \quad x \in R^n \tag{15}$$

where $\{\psi_i\}$ is the set of Hermite polynomial functions of the Gaussian random variables ξ.
The model state error covariance matrix is given by

$$P = \sum_{i=1}^{P} x_i x_i^T \langle \psi_i^2 \rangle \quad P \in R^{n\times n} \tag{16}$$

where the operator $\langle . \rangle$ represents the expected value.
Given a measurements vector d, its polynomial chaos representation is as follows

$$d = \sum_{i=0}^{P} d_i\psi_i\big(\xi(\theta)\big) \quad d \in R^m \tag{17}$$

where m is the total number of measurements, d_0 is the mean, given from the actual measurement vector, and $\{d_1, \ldots, d_P\}$ are the measurement uncertainties. The polynomial chaos representation of d can be stored in matrix B

$$B = (d_0, d_1, \ldots, d_P) \quad B \in R^{m\times(P+1)} \tag{18}$$

The measurement error covariance matrix can then be represented as

$$R = \sum_{i=1}^{P} d_i d_i^T \langle \psi_i^2 \rangle \quad R \in R^{m\times m} \tag{19}$$

The analysis or corrector step is stated as follows

$$A^a = A^f + KG(B - HA^f) \tag{20}$$

where H is the observation matrix and KG is the Kalman gain, having the same formulation as the one used in the standard KF

$$KG = P^f H^T (HP^f H^T + R)^{-1} \tag{21}$$

To avoid the curse of dimensionality due to the incorporation of temporal independent sources of uncertainty of the model errors and measurement errors in the PCKF framework, the practical implementation scheme of PCKF presented in (Slika and Saad 2016, 2017) is adopted in this study. This scheme relies on limiting the PCE bases to finite number of terms to keep the computational cost minimal yet without scarifying the accuracy of the filter. In this setting, once the allocated dimensions for model error and/or measurement error are utilized, the error covariance Pa is projected on a first order PCE with only M_p dimensions, to be able to represent additional uncertainties, as demonstrated below

Before projection

$$u(x,\theta) \approx \sum_{i=0}^{P} u_i(x)\psi_i\big(\xi(\theta)\big) \tag{22}$$

$$P_a = \sum_{i=1}^{P} u_i u_i^T < \psi_i^2 > \tag{23}$$

After projection

$$u(x,\theta) \approx \sum_{j=0}^{P} u'_j(x)\psi_j\big(\xi(\theta)\big), where \tag{24}$$

$$u'_0 = u_0 \; and \; u'_j = 0 \; if \; j > M_p \tag{25}$$

Estimating the set of coefficients $\{u'_i\}_1^{M_p}$ requires solving the system of non-linear equations outlined above. Given a state vector of size n, then the number of unknowns is $M_p \times n$, and the number of equations is n^2. Therefore M_p must be equal at least to n, to guarantee a solution for the nonlinear system of equations. With such relaxed formulation, having the number of equations less than the unknown parameters, the system of equations could have multiple solutions. Usually the solution is estimated, up to a pre-specified tolerance, in the neighborhood of a specified initial guess, which in this case could be the set of u_j's with the highest contribution to the covariance matrix (Slika and Saad 2017).

3. Numerical example

The numerical problem consists of four-degrees of freedom system, as shown in Fig. 1 subjected to El-Centro Earthquake ground excitation. A pre-defined damage of the first DOF is imposed 10 seconds after the excitation hits the system. Additionally, all DOFs are assumed to undergo hysteretic behaviors characterized by the Bouc-Wen model. The mass for each DOF is assumed to be equal such that $M_1 = M_2 = M_3 = M_4 = 2\,Kg$ (Ghanem and Ferro 2006, Chatzi and Smyth 2009, Saad and Ghanem 2011).

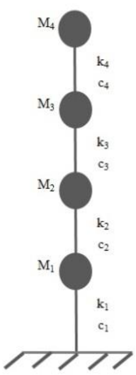

Fig. 1 Model of the four-DOF System

The displacements and velocities of the different DOFs of the system are assumed to be monitored at all times. The performance and robustness of both the non-intrusive ensemble Kalman filter and the intrusive polynomial chaos Kalman filter methods are tested on this numerical problem through the estimation of the displacement and velocity of each DOF as well as the system's unknown parameters.

The system dynamics are mathematically represented by the following equation of motion

$$M\ddot{u} + C\dot{u}(t) + \propto K_{el}u(t) + (1-\propto)K_{in}z(x,t) = -M\tau\ddot{u}_g(t) \tag{26}$$

$$\begin{bmatrix} M_1 & 0 & 0 & 0 \\ 0 & M_2 & 0 & 0 \\ 0 & 0 & M_3 & 0 \\ 0 & 0 & 0 & M_4 \end{bmatrix}\begin{bmatrix} \ddot{u}_1 \\ \ddot{u}_2 \\ \ddot{u}_3 \\ \ddot{u}_4 \end{bmatrix} + \begin{bmatrix} c_1+c_2 & -c_2 & 0 & 0 \\ -c_2 & c_2+c_3 & -c_3 & 0 \\ 0 & -c_3 & c_3+c_4 & -c_4 \\ 0 & 0 & -c_4 & c_4 \end{bmatrix}\begin{bmatrix} \dot{u}_1 \\ \dot{u}_2 \\ \dot{u}_3 \\ \dot{u}_4 \end{bmatrix} + \propto \begin{bmatrix} k_1+k_2 & -k_2 & 0 & 0 \\ -k_2 & k_2+k_3 & -k_3 & 0 \\ 0 & -k_3 & k_3+k_4 & -k_4 \\ 0 & 0 & -k_4 & k_4 \end{bmatrix}\begin{bmatrix} u_1 \\ u_2 \\ u_3 \\ u_4 \end{bmatrix} + (1-\propto)\begin{bmatrix} k_1+k_2 & -k_2 & 0 & 0 \\ -k_2 & k_2+k_3 & -k_3 & 0 \\ 0 & -k_3 & k_3+k_4 & -k_4 \\ 0 & 0 & -k_4 & k_4 \end{bmatrix}\begin{bmatrix} z_1 \\ z_2 \\ z_3 \\ z_4 \end{bmatrix} = \begin{bmatrix} F_1(t) \\ F_2(t) \\ F_3(t) \\ F_4(t) \end{bmatrix} \tag{27}$$

where M is the mass matrix, C is the damping matrix, K_{el} and K_{in} are respectively the elastic and inelastic stiffness matrices and are both assumed to be equal to the ordinary stiffness matrix of the system, $\propto$ is the ratio of the post yielding stiffness to the elastic stiffness and is taken to be equal to 0.15 for this special numerical problem, τ is an influence vector, u is the displacement vector and z is the evolutionary hysteretic vector of dimension n and whose ith component is expressed by the Bouc-Wen model by (Ghanem and Ferro 2006, Chatzi and Smyth 2009, Saad and Ghanem 2011)

$$\dot{z}_i = A_i\dot{x}_i - \beta_i|\dot{x}_i||z_i|^{n_i-1}z_i - \gamma_i\dot{x}_i|z_i|^{n_i} \qquad i = 1,\dots,n \tag{28}$$

where $A = 1$, x is the inter-story drift vector and $\beta, n \; and \; \gamma$ are the Bouc-Wen hysteretic model parameters. Parameter n is taken to be equal to 1 for simplicity reasons to avoid using Taylor series approximations for the power of a non-polynomial for the PCKF method. The purpose of this numerical problem is to identify the states of the system as well as the parameters $\beta_i, \gamma_i, k_i \; and \; c_i$, where $i = 1,\dots,4$ is the number of degrees of freedom.

To synthetically generate the measured data, the stiffness is assumed to be constant and equal to $k = 8.5\,N/m$ on all DOFs, the damping is also assumed to be constant for all DOFs such that $c = 0.27$, and the values of the Bouc-Wen hysteretic parameters, before the damage occurs at the first DOF of the system, are assumed to be $\beta_1 = \beta_2 = \beta_3 = \beta_4 = 2\ and\ \ \gamma_1 = \gamma_2 = \gamma_3 = \gamma_4 = 1$ (Chatzi and Smyth 2009). An increase of 50% to the values of hysteretic parameters of the first DOF is added once the damage is imposed to create a softening character(Shen *et al.* 2005). Therefore, the values of $\beta\ and\ \gamma$ of the first DOF ten seconds after the excitation hits the system under consideration become $\beta_1 = 3\ and\ \gamma_1 = 1.5$. Measurements are assumed to available every 20 time steps with a fixed time step dt = 0.01 seconds. It should be noted that a sensitivity analysis was performed to select this time step value. An additive Gaussian white noise perturbation with a standard deviation equals to 5% of the exact data is added to the simulated displacements and velocities of the system's DOFs to represent the measurement errors. The fourth-order Runge-Kutta integration scheme is used to solve the differential Eq. (27) to determine the system responses of the displacements and velocities.

For data assimilation purposes, the state variable vector and its first order derivative are respectively represented in the following two equations as

$$X = \begin{bmatrix} u_1 \\ u_2 \\ u_3 \\ u_4 \\ \dot{u}_1 \\ \dot{u}_2 \\ \dot{u}_3 \\ \dot{u}_4 \\ z_1 \\ z_2 \\ z_3 \\ z_4 \\ \beta_1 \\ \beta_2 \\ \beta_3 \\ \beta_4 \\ \gamma_1 \\ \gamma_2 \\ \gamma_3 \\ \gamma_4 \\ k \\ c \end{bmatrix} \tag{29}$$

$$\dot{X} = \begin{bmatrix} \dot{X}_1 \\ \dot{X}_2 \\ \dot{X}_3 \\ \dot{X}_4 \\ \dot{X}_5 \\ \dot{X}_6 \\ \dot{X}_7 \\ \dot{X}_8 \\ \dot{X}_9 \\ \dot{X}_{10} \\ \dot{X}_{11} \\ \dot{X}_{12} \\ \dot{X}_{13} \\ \dot{X}_{14} \\ \dot{X}_{15} \\ \dot{X}_{16} \\ \dot{X}_{17} \\ \dot{X}_{18} \\ \dot{X}_{19} \\ \dot{X}_{20} \\ \dot{X}_{21} \\ \dot{X}_{22} \end{bmatrix} = \begin{bmatrix} \dot{u}_1 \\ \dot{u}_2 \\ \dot{u}_3 \\ \dot{u}_4 \\ \ddot{u}_1 \\ \ddot{u}_2 \\ \ddot{u}_3 \\ \ddot{u}_4 \\ \dot{z}_1 \\ \dot{z}_2 \\ \dot{z}_3 \\ \dot{z}_4 \\ \dot{\beta}_1 \\ \dot{\beta}_2 \\ \dot{\beta}_3 \\ \dot{\beta}_4 \\ \dot{\gamma}_1 \\ \dot{\gamma}_2 \\ \dot{\gamma}_3 \\ \dot{\gamma}_4 \\ \dot{k} \\ \dot{c} \end{bmatrix} \tag{30}$$

$$\dot{X} = \begin{bmatrix} X_5 \\ X_6 \\ X_7 \\ X_8 \\ -\frac{1}{M_1}\begin{bmatrix} -\ddot{u}_g + (X_{17} + X_{18})X_5 - X_{18}X_6 \\ +\alpha[(X_{13} + X_{14})X_1 - X_{14}X_2] \\ +(1-\alpha)[(X_{13} + X_{14})X_9 - X_{14}X_{10}] \end{bmatrix} \\ -\frac{1}{M_2}\begin{bmatrix} -\ddot{u}_g - X_{18}X_5 + (X_{18} + X_{19})X_6 - X_{19}X_7 \\ +\alpha[-X_{14}X_1 + (X_{14} + X_{15})X_2 - X_{15}X_3] \\ +(1-\alpha)[-X_{14}X_9 + (X_{14} + X_{15})X_{10} - X_{15}X_{11}] \end{bmatrix} \\ -\frac{1}{M_3}\begin{bmatrix} -\ddot{u}_g - X_{19}X_6 + (X_{19} + X_{20})X_7 - X_{20}X_8 \\ +\alpha[-X_{15}X_2 + (X_{15} + X_{16})X_3 - X_{16}X_4] \\ +(1-\alpha)[-X_{15}X_{10} + (X_{15} + X_{15})X_{11} - X_{16}X_{12}] \end{bmatrix} \\ -\frac{1}{M_4}\begin{bmatrix} -\ddot{u}_g - X_{20}X_7 + X_{20}X_8 \\ +\alpha[-X_{16}X_3 + X_{16}X_4] \\ +(1-\alpha)[-X_{16}X_{11} + X_{16}X_{12}] \end{bmatrix} \\ X_5 - X_{13}|X_5|X_9 - X_{17}X_5|X_9| \\ X_6 - X_{14}|X_6|X_{10} - X_{18}X_6|X_{10}| \\ X_7 - X_{15}|X_7|X_{11} - X_{19}X_7|X_{11}| \\ X_8 - X_{16}|X_8|X_{12} - X_{20}X_8|X_{12}| \\ 0 \\ 0 \\ 0 \\ 0 \\ 0 \\ 0 \\ 0 \\ 0 \\ 0 \\ 0 \end{bmatrix} \tag{31}$$

where $\ddot{u}_g$ is the El-Centro earthquake ground excitation.

For both filters, the EnKF and the PCKF methods, the inverse model that is used to detect the behavior of the system under consideration is also expressed by the Bouc-Wen model.

The initial values of the displacements u_i, velocities $\dot{u}_i$ and evolutionary hysteretic vector z_i $(i = 1, \dots, 4)$ are assumed to be the following

$$\begin{gathered} u_1^0 = u_2^0 = u_3^0 = u_4^0 = 0; \\ \dot{u}_1^0 = \dot{u}_2^0 = \dot{u}_3^0 = \dot{u}_4^0 = 0; \\ and\ z_1^0 = z_2^0 = z_3^0 = z_4^0 = 0 \end{gathered} \tag{32}$$

The initial guesses of the unknown parameters of the system are assumed to have the following mean values

$$\begin{gathered} \beta_1^0 = 2.5;\ \beta_2^0 = 2.5;\ \beta_3^0 = 2.5;\ \beta_4^0 = 2.5; \\ \gamma_1^0 = 1.2;\ \gamma_2^0 = 1.2;\ \gamma_3^0 = 1.2;\ \gamma_4^0 = 1.2; \\ k^0 = 7\ and\ c^0 = 0.4 \end{gathered} \tag{33}$$

and a standard deviation of 10% of the initial assumptions.

A fourth order Runge-Kutta time integrating method is implemented once again to propagate the system state forward in time. An additive Gaussian white noise having a standard deviation equals to 2.5% of the forecasted state vector and 5% of the forecasted parameters, is used every 5 time steps to represent the model uncertainty. The perturbed synthetic measurements of the displacements and velocities of the DOFs are used to calibrate the model parameters and estimate the response of the system under consideration.

For the PCKF method, the Galerkin projection method is used to solve Eq. (27) to determine the acceleration $\ddot{u}_i$ $(i = 1, \dots, 4)$. The Galerkin method is based on projection and is used to approximate solutions of differential equations. On the other hand, to solve Eq. (28)

and determine the evolutionary hysteretic vector z_i ($i = 1, \dots, 4$), the Galerkin projection cannot be used because of the presence of the absolute value in the equation. Therefore, a linear fitting method (i.e., regression method) is used instead to solve Eq. (28).

4. Uncertainty quantification

As previously noted, development of SHM frameworks for complex nonlinear systems is accompanied by the presence of many sources of randomness. One major cause of uncertainty is the use of mathematical and numerical models to simulate the true physics of the system, and therefore leading to the creation of model errors coming from the inability of such models to adequately describe the system's real behavior. Another main source of error is the measurement uncertainty that is due to the restricted ability of the measurement data to accurately describe the real observations. Parametric variability is an additional source of randomness coming from the limited knowledge about the exact values of the system's input parameters.

The different sources of randomness in modeling physical phenomena can be classified into two main categories, aleatoric and epistemic uncertainty (Helton 2000, Helton and Davis 2002, Ghanem and Spanos 2003, Helton and Oberkampf 2004, Der Kiureghiana and Ditlevsen 2009). The first category is due to natural randomness inherent in the behavior or environment of the system. The aleatoric uncertainty is also called irreducible uncertainty since it cannot be reduced by performing more experimental testing. In the presented numerical problem, this class of uncertainty is primarily detected in the input variables and parameters ($\beta_i, \gamma_i, k\ and\ c$) whose exact values are unpredictable. The second category, the epistemic uncertainty or reducible uncertainty, is mainly due to the lack of knowledge and available observational data. It can be reduced by conducting additional experimental studies or implementing a new better physical model, leading to an increased amount of knowledge about the behavior of the system under consideration. This category of uncertainty is detected in the numerical problem under consideration through the model errors that are associated with each state ($u_i, \dot{u}_i\ and\ z_i$), and that are implemented to account for the simplifications in the mathematical models used to roughly represent the true physical state of the system. This reducible uncertainty is also spotted in the synthetic measured displacements and velocities of the different DOFs of the system and their restricted capacities to replicate the true observed data.

4.1 Representation of the different sources of uncertainty

For highly nonlinear systems that are subjected to many independent sources of errors, the EnKF requires a large ensemble size to properly estimate the system states and unknown parameters and to accurately detect and locate the damage. Therefore it is expected that a relatively large ensemble is required for the EnKF approach to acceptably identify the unknown states and variables of the 4-DOF system under consideration.

On the other hand, regarding the PCKF method, the dimension is specified based on the number of independent sources of uncertainty available in the system under consideration. Therefore, one major challenge faced by the authors was the increase in the dimensionality of the PCE due to the presence of different independent sources of uncertainties, i.e., every time a measurement is recorded or a model error is implemented in the system to account for the physical and mathematical model simplifications, an additional increase in the dimensionality of the PCE is incorporated. To approach this problem, the PCKF implementation in (Slika and Saad 2016, 2017) is adopted where it maintains an accurate approximation of the covariance yet it limits the number of the required PCE terms or dimensions. Therefore, it overcomes the curse of dimensionality due to the incorporation of temporal independent sources of uncertainties at a cost of solving a nonlinear system of equations.

In the problem at hand, the errors due to model uncertainty are assumed to be correlated for each state ($u, \dot{u}\ and\ z$) and for the parameters $c\ and\ k$, whereas the errors representing the model uncertainties in $\beta\ and\ \gamma$ are respectively assumed to be independent, resulting in a total of 13 independent sources of model errors. Next, the errors due to measurement uncertainties are also assumed to be respectively correlated for u and $\dot{u}$, leading to two additional independent sources of errors. Finally, the initial guess errors are taken to be correlated for each parameter ($\beta, \gamma, c\ and\ k$) respectively, resulting in 4 additional independent sources of errors. Table 1 presents further clarifications about the total number of independent sources of uncertainty adopted in this numerical example.

In the adopted practical implementation scheme, the number of dimensions M is made up of two parts M_p and M_f. The M_p dimensions are allocated to handle the projected covariance matrix such that M_p is at least equal to n, the length of state vector, which is 22 in this case, while the M_f dimensions are allocated to handle at least one addition of model error and measurement error after the projection (Slika and Saad 2016, 2017).

Table 1 Total number of independent sources of Uncertainty

Independent Sources of Errors	**Model Error**	**Measurement Error**	**Initial Guess Error**
$\boldsymbol{u_i}$	1	1	0
$\boldsymbol{\dot{u}_i}$	1	1	0
$\boldsymbol{z_i}$	1	0	0
$\boldsymbol{\beta_i}$	4	0	1
$\boldsymbol{\gamma_i}$	4	0	1
$\boldsymbol{k}$	1	0	1
$\boldsymbol{c}$	1	0	1
Total	**13**	**2**	**4**

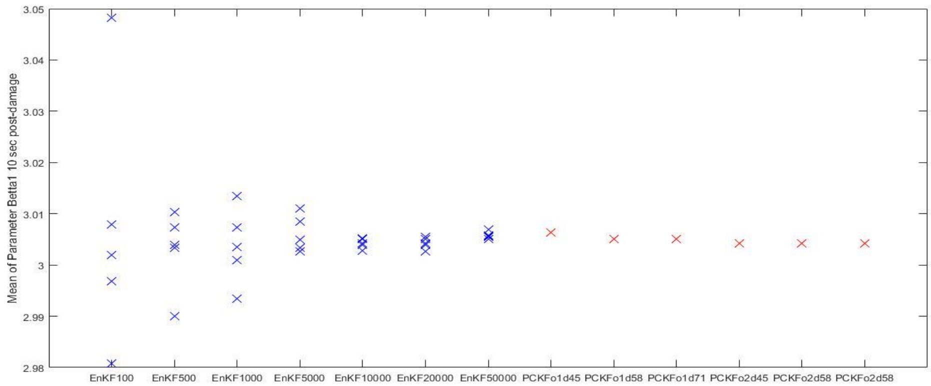

Fig. 2 Mean of predicted parameter $\beta 1$ vs. Ensemble size and PCKF dimension and order, 10 seconds after the damage

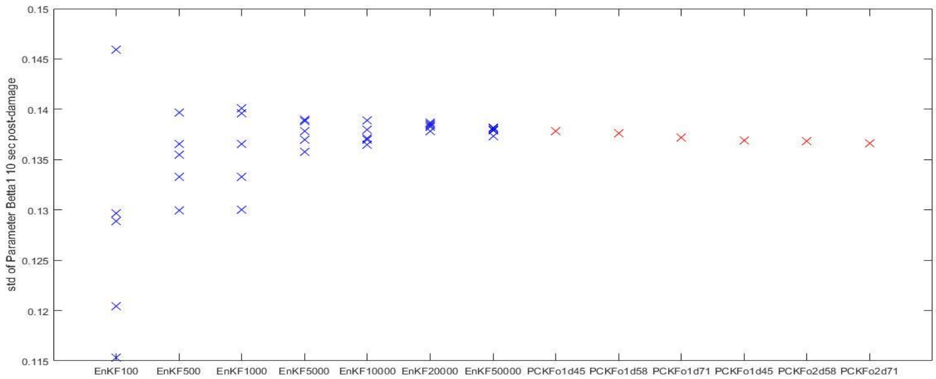

Fig. 3 Standard deviation of predicted parameter $\beta 1$ vs. Ensemble size and PCKF dimension and order, 10 seconds after the damage

Therefore, in accordance with the above problem formulation, the minimum number of dimensions in this study is found to be equal to 45 (i.e., a minimum of 3 finite terms is taken for the model error (13×3), 1 finite term for the measurement error(2×1), and no additional terms for the initial guess errors; therefore the total number of PCE dimensions becomes: $13 \times 3 + 2 \times 1 + 4 = 45)$.

5. Results and discussions

Before proceeding with the results, it should be noted that sensitivity analyses on the ensemble size of the EnKF method and on the order and dimension of the PCKF method were performed. For this purpose, the mean of the predicted hysteretic parameter $\beta 1$ and its standard deviation ten seconds after the damage is imposed on the first DOF are calculated for different ensemble sizes for the EnKF approach and different orders and dimensions for the PCKF method. While the PCKF method gives the same outcomes for different simulation runs having same order and dimension of the PCE, the results of the EnKF method slightly vary between different simulation runs for the same ensemble size. For this reason, five simulation runs were respectively executed for each ensemble size. Figs. 2 and 3 respectively represent the values of the mean and standard deviation of the predicted parameter $\beta 1$ at ten seconds post-damage, calculated using the EnKF and PCKF approaches.

It can be seen from Fig. 2 that as the ensemble size increases, the variability between the means of the predicted parameters $\beta 1$ of the different simulation runs decreases to attain an acceptable variability for a 10,000 ensemble size, in addition to a relatively small percentage error (around 0.05% error) if compared to a benchmark problem based on a sufficiently large ensemble size equals to 250,000 ensemble. This observation is also valid for Fig. 3, where the results of the standard deviations of the predicted parameters $\beta 1$, at ten seconds after the damage is imposed on the first DOF, attain acceptable variability between different simulation runs for an EnKF with 10,000 ensemble size and a small percentage error (around 0.6% error) when compared to the benchmark problem with 250,000 ensemble size.

Similarly, as the order of the PCKF method is increased from 1 to 2, the method results in a closer approximation of the mean of the parameter $\beta 1$ to the assumed exact measured value, as shown in Fig. 2, and in a slightly smaller standard deviation of parameter $\beta1$, as shown in Fig. 3. In addition, for PCKF order 2, a rough plateau in the values of the mean and standard deviation of parameter $\beta1$ is noticeable for different dimensions of the PCE. This is due to the new implementation of the PCKF method that maintains the covariance even for low dimensional PCE.

The PCE with order 2 and dimension 45 recorded low percentage errors (around 0.019% for the mean of parameter $\beta1$ and 0.01% errors for the standard deviation of parameter $\beta1$) when compared to the benchmark problem based on 250,000 ensemble size, therefore the PCKF with order 2 and dimension 45 plays the role of a good parameter estimator. As a conclusion, an EnKF with 10,000 ensemble size and a PCE with order 2 and dimension 45 can be used for the comparative study in this numerical problem.

Furthermore, while the duration for the PCKF parameter and state identification with dimension 45 and order 2 was 3.0618x103 seconds, the computational time for the EnKF identification with size 10,000 ensembles of realizations was 7.1455x103 seconds on the same machine. As a result, for high accuracy requirements, while both filters are able to approximate the system state and unknown parameters and identify the damage in space and time, the PCKF method outperforms the EnKF approach, that requires high ensemble size to attain high precisions, in terms of computational expenses.

Figs. 4-7 respectively represent for each DOF, a comparison between the EnKF and PCKF estimates of the displacement (part (a) of each figure), velocity (part (b) of each figure) and evolutionary hysteretic vector (part (c) of each figure), and their respective synthetic actual measured values. It can be clearly seen that there is a very good match between the three plots in each figure, which implies that both variations of the Kalman filter method play the role of very good estimators of the system state.

The EnKF and PCKF estimates of the hysteretic model parameters β and γ of each DOF are respectively presented in Figs. 8 and 9.

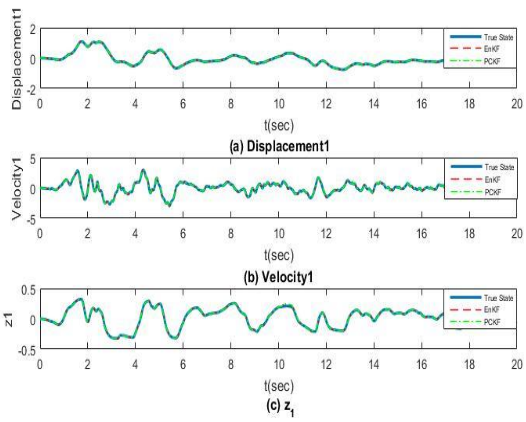

Fig. 4 EnKF and PCKF estimates of First DOF displacement, velocity and evolutionary hysteretic

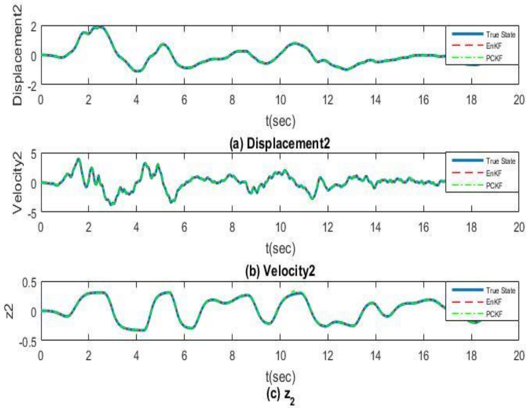

Fig. 5 EnKF and PCKF estimates of Second DOF displacement, velocity and evolutionary hysteretic

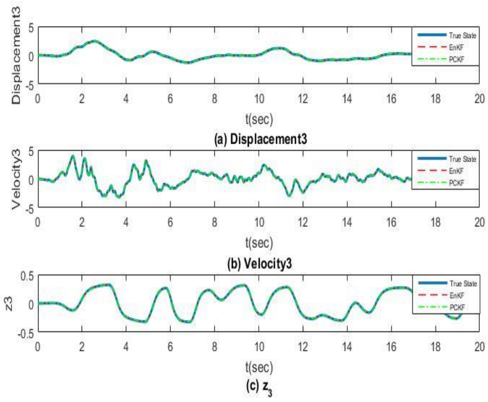

Fig. 6 EnKF and PCKF estimates of Third DOF displacement, velocity and evolutionary hysteretic vector

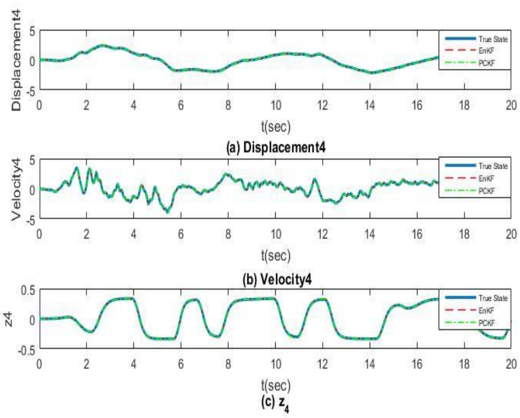

Fig. 7 EnKF and PCKF estimates of Fourth DOF displacement, velocity and evolutionary hysteretic

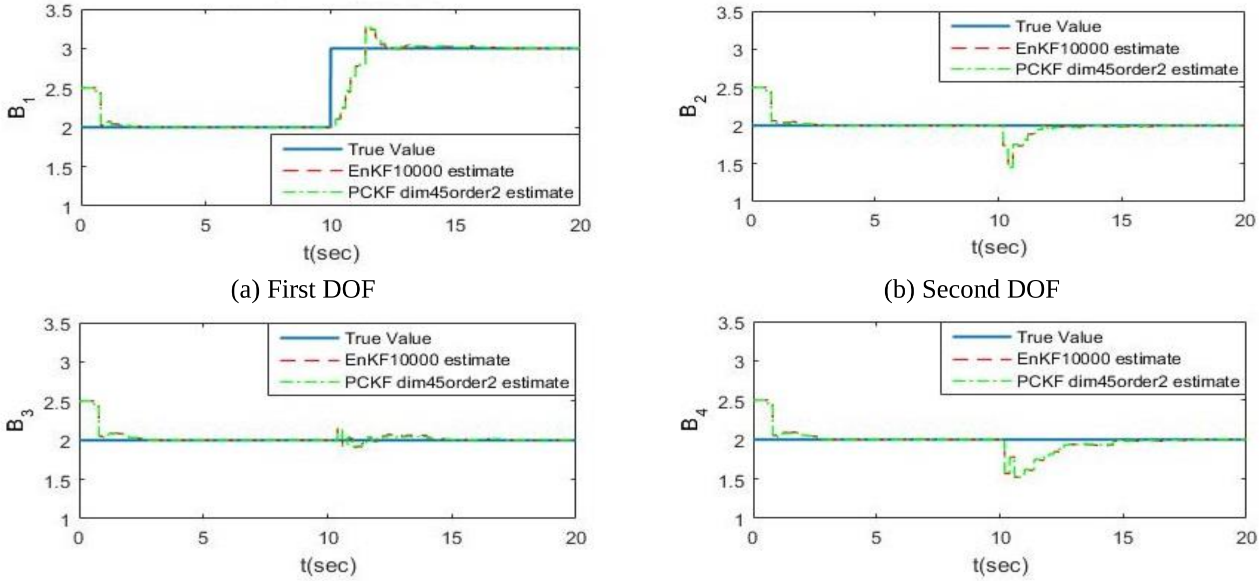

(a) First DOF (b) Second DOF

(c) Third DOF (d) Fourth DOF

Fig. 8 EnKF and PCKF estimates of Parameter β

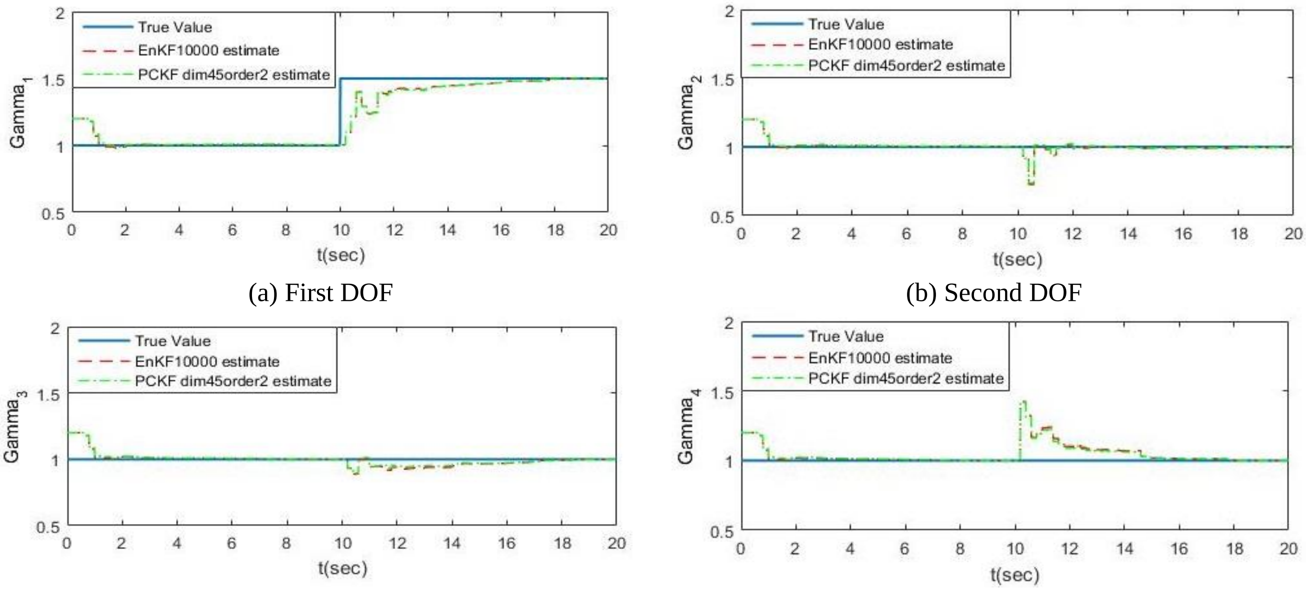

(a) First DOF (b) Second DOF

(c) Third DOF (d) Fourth DOF

Fig. 9 EnKF and PCKF estimates of Parameter γ

A perfect match between the EnKF and PCKF estimates of the different hysteretic model parameters can be obviously noticed in each figure. Furthermore, both filter variations were able to locate the imposed damage in time and space, which is represented by the jump of the different parameters at 10 seconds, followed by a correction and matching with the true values after few time steps.

Same conclusions can be drawn for parameter k, represented in Fig. 10 part (a) and parameter c, represented in Fig. 10(b). Both filters were able to estimate the true values of parameters k and c, even when starting from relatively far initial guess values, and to locate the damage imposed 10 seconds after the excitation hits the system under consideration.

Fig. 11 represents the hysteretic loop corresponding to the first DOF. The nearly perfect match between the actual hysteretic loop and its EnKF and PCKF estimates authenticates the validity of parameter approximation of both filters.

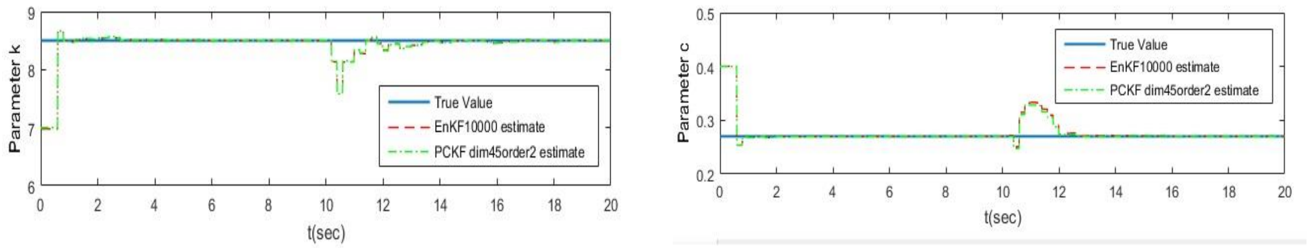

(a) Parameter k (b) Parameter c

Fig. 10 EnKF and PCKF estimates of Parameters k and c

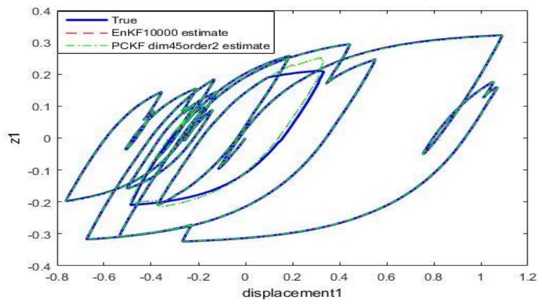

Fig. 11 Hysteresis Loop of the first DOF

6. Conclusions

In the present work, the importance of uncertainty quantification is highlighted through a comparative study between intrusive and non-intrusive techniques used to quantify and represent the available uncertainties. For this reason, a comparison between two different variations of the Kalman filter technique, Ensemble Kalman Filter and Polynomial Chaos Kalman Filter, is performed. The comparison is based on the computational burden of the simulation runs required by each method to identify the system state and parameters and on the accuracy and performance of each filter in quantifying the uncertainty for SHM purposes. This is illustrated through a numerical example, consisting of a 4-degrees of freedom nonlinear system subjected to seismic excitation and suffering from hysteretic behaviors represented by the Bouc-Wen model. A pre-defined damage of the first degree of freedom is imposed ten seconds after the excitation hits the system.

A sensitivity analysis was performed on the ensemble size for the EnKF method and a relatively large ensemble size equals to 10,000 was selected to attain a sufficiently high accuracy in estimating the parameters and response of this complex and highly nonlinear system for damage detection purposes. On the other hand, an exhaustive analysis was performed on the dimensionality of the PCE used that is increased every time an independent source of error, due to model or measurement uncertainty, is incorporated in the system. For this reason, the PCE bases were limited to finite terms while maintaining a good approximate propagation of the covariance matrix, resulting in a minimum dimension equals to 45 for the PCKF method. This minimum dimension of the PCE was used along with an order equals to 2 in the comparative analysis.

While both variations of the Kalman filter method were able to locate the damage in space and time and to accurately approximate the system state and unknown parameters for SHM purposes, the PCKF method outperformed the ordinary EnKF approach in terms of computational effort. The underlying reason behind the adequate performance of both filters is that they both properly account for all sources of uncertainty in their formulation. If that was not the case, and an engineer decided to use a lower order filter formulation, the rendered filter outcome will not be useful.

As a conclusion, since the EnKF belongs to the class of non-intrusive methods that use black-box models to solve forward problems, it is easier to implement if compared to the intrusive methods such as the PCKF approach that requires going through the black-box model and modifying the equations to account for the polynomial chaos representations of the unknown variables. On the other hand, for highly nonlinear and complex systems, the EnKF approach requires a relatively large ensemble size to attain a comparable high accuracy with the PCKF method and consequently a higher computational burden. Therefore, the optimal sequential data assimilation framework is a trade-off between ease of use, numerical accuracy and computational burden. Based on the complexity of the mathematical model and the nature of the existing sources of uncertainty, the user can choose whether to adopt an intrusive or non-intrusive technique for handling the problem at hand.

One limitation of this study is that the drawn conclusions, although valueable, are based on synthetic data. Future plans include applying the two filters on real life problems and assessing their adequacy accordingly.

References

Al-Hussein, A. and Haldar, A. (2016), “Unscented Kalman filter with unknown input and weighted global iteration for health assessment of large structural systems”, *Struct. Control Health Monit.*, **23**(1), 156-175.

Arasaratnam, I. and Haykin, S. (2009), “Cubature Kalman filters”, *IEEE T. Autom. Control*, **54**(6), 1254-1269.

Bertino, L., Evensen, G. and Wackernagel, H. (2003), “Sequential data assimilation techniques in oceanography”, *International Stat. Rev.*, **71**(2), 223-241.

Burgers, G., Leeuwen, P. and Evensen, G. (1998), “Analysis scheme in the ensemble Kalman filter", *Mon. Weather Rev.*, **126**(6), 1719-1724.

Chang, P., Faltau, A. and Liu, S. (2003), "Review Paper: health monitoring of civil infrastructure", *Struct. Health Monit.*, **2**(2), 257-267.

Chatzi, E.N. and Smyth, A.W. (2009), "The unscented Kalman filter and particle filter methods for nonlinear structural system identification with non-collocated heterogeneous sensing", *Struct. Control Health Monit.*, **16**(1), 99-123.

Chatzi, E.N. and Smyth, A.W. (2013), "Particle filter scheme with mutation for the estimation of time-invariant parameters in structural health monitoring applications", *Struct. Control Health Monit.*, **20**(7), 1081-1095.

Chatzi, N. and Fuggini, C. (2015), "Online correction of drift in structural identification using artificial white noise observations and an unscented Kalman filter", *Smart Struct. Syst.*, **16**(2), 295-328.

Chowdhary, G. and Jategaonkar, R. (2010), "Aerodynamic parameter estimation from flight data applying extended and unscented Kalman filter", *Aerosp. Sci. Technol.*, **14**(2), 106-117.

Chui, C. and Chen, G. (1991), *Kalman Filtering with Real Time Applications*, Springer.

Corigliano, A. and Mariani, S. (2004), "Parameter identification in explicit structural dynamics: performance of the ectended Kalman filter", *Comput. Method. Appl. M.*, **193**(36), 3807-3835.

Daley, R. (1997), "Atmospheric data assimilation", *J. Meteorol. Soc. Japan Series 2*, **75**, 319-329.

Der Kiureghiana, A. and Ditlevsen, O. (2009), "Aleatory or epistemic? Does it matter? ", *Struct. Saf.*, **31**(2), 105-112.

Doebling, S., Farrar, C., Prime, M. and Shevitz, D. (1996), Damage identification and health monitoring of structural and mechanical systems from changes in their vibration characteristics: a literature review, Los Alamos National Lab., NM (United States).

Evensen, G. (1994), "Sequential data assimilation with a nonlinear quasi-geostrophic model using Monte Carlo to forecast error statistics", *J. Geophysical Research: Oceans (1978-2012)*, **99**(C5), 10143-10162.

Evensen, G. (2003), "The ensemble Kalman filer: Theoretical formulation and practical implementation", *Ocean Dynam.*, **53**(4), 343-367.

Evensen, G. (2009), "The ensemble Kalman filter for combined state and parameter estimation", *IEEE Control Syst. Mag.*, 83-104.

Farrar, C. and Worden, K. (2007), "An introduction to structural health monitoring", *Philosophical Transactions of the Royal Society A: Mathematical, Physical and Engineering Sciences*, **365**(1851), 303-315.

Ghanem, R. (1999), "Ingredients for a general purpose stochastic finite element formulation", *Comput. Method. Appl. M.*, **168**(1), 19-34.

Ghanem, R. and Ferro, G. (2006), "Health monitoring of strongly nonlinear systems using the ensemble Kalman filter", *Struct. Control Health Monit.* **13**(1), 245-259.

Ghanem, R. and Spanos, P. (2003), *Stochastic Finite Elements: A Spectral Approach*, Courrier Corporation.

Gillijns, S., Mendoza, O., Chandrasekar, J., De Moor, B., Bernstein, D. and Ridley, A. (2006), "What is the ensemble Kalman filter and how well does it work?", *Proceedings of the American Control Conference*, Minneapolis.

Goyal, D. and Pabla, B.S. (2015), "The vibration monitoring methods and signal processing techniques for structural health monitoring: a review", *Arch. Comput. Method. E.*, 1-10.

Grewal, M. and Andrews, A. (2008), *Kalman Filtering Theory and Applications using MATLAB*, John Wiley & Sons.

Hassani, V., Tjahjowidodo, T. and Do, T.N. (2014), "A survey in hysteresis modeling, identification and control", *Mech. Syst. Signal Pr.*, **49**(1), 209-233.

Helton, J.C. (2000), "Sampling-based methods for uncertainty and sensitivity analysis", *Multimedia Environ. Model.*, **32**(2), 73.

Helton, J.C. and Davis, F.J. (2002), "Illustration of sampling-based methods for uncertainty and sensitivity analysis", *Risk Anal.*, **22**(3), 591-622.

Helton, J.C. and Oberkampf, W.L. (2004), "Alternative representations of epistemic uncertainty", *Reliab. Eng. Syst. Saf.*, **85**(1), 1-10.

Hommels, A., Murakami, A. and Nishimura, S.I. (2009), "A comparison of the ensemble Kalman filter with the Unscented Kalman filter: application to the construction of a raod embankment", *Geotechniek*, **13**(1), 52.

Ikhouane, F., Mañosa, V. and Rodellar, J. (2007), "Dynamic properties of the hysteretic Bouc-Wen model", *Syst. Control. Lett.*, **56**(3), 197-205.

Ismail, M., Lkhouane, F. and Rodellar, J. (2009), "The hysteresis Bouc-Wen model, a survey", *Arch. Omputat. Method. Eng.*, **16**(2), 161-188.

Kalman, R. (1960), "A new approach to linear filtering and prediction problems", *J. Basic Eng.*, **82**(1), 35-45.

Kalnay, E. (2003), *Atmospheric Modeling, Data Assimilation and Predictability*, Cambridge University Press.

Kandepu, R., Foss, B. and Imsland, L. (2008), "Applying the unscented Kalman filter for nonlinear state estimation", *J. Process Contr.*, **18**(7), 753-768.

LeDimet, F. and Talagrand, O. (1986), "Variational algorithms for analysis and assimilation of meteorological observations: Theoretical aspects", *Tellus A*, **38**(2), 97-110.

Lei, Y., Chen, F. and Zhou, H. (2015), "A two-stage and two-step algorithm for the identification of structural damage and unknown excitations: numerical and experimental studies", *Smart Struct. Syst.*, **15**(1), 57-80.

Li, J. and Xiu, D. (2009), "A generazlized polynomial chaos based ensemble Kalman filter with high accuracy", *J. Comput. Phys.*, **228**(15), 5454-5469.

Liu, L., Lei, Y. and He, M. (2015), "Locating and identifying model-free structural nonlinearities and systems using incomplete measured structural responses", *Smart Struct. Syst.*, **15**(2), 409-424.

Navon, I., Zou, X., Derber, J. and Sela, J. (1992), "Variational data assimilation with an adiabatic version of the NMC spectral model", *Am. Meterol. Soc.*, **120**(7), 1433-1446.

Saad, G. (2007), "Stochastic data assimilation with application to multi-phase flow and health monitoring problems", *ProQuest*.

Saad, G. and Ghanem, R. (2009), "Characterization of reservoir simulation models using a polynomial chaod-based ensemble Kalman filter", *Water Resour. Res.*, **45**(4).

Saad, G. and Ghanem, R. (2011), "Robust structural health monitoring using a polynomial chaos sequential data assimilation technique", *Proceedings of the COMPDYN 2011*, Corfu, Greece.

Saad, G., Ghanem, R. and Masri, S. (2007), "Robust system identification of strongly non-linear dynamics using a polynomial chaos based sequential data assimilation technique", *Proceedings of the 48th AIAA/ASME/ASCE/AHS/ASC Structures, Structural Dynamics and Materials Conference*, Honolulu.

Shen, Y., Golnaraghi, M.F. and Heppler, G.R. (2005), "Analytical and experimental study of the response of a suspension system with a magnetorheological damper", *J. Intel. Mat. Syst. Str.*, **16**(2), 135-147.

Slika, W. and Saad, G. (2016), "An ensemble Kalman filter approach for service life prediction of reinforced concrete structures subject to chloride-induced corrosion", *Constr. Build. Mater.*, **115**, 132-142.

Slika, W. and Saad, G. (2016), "A robust polynomial chaos Kalman filter framework for corrosion detection in reinforced concrete structures", *Proceedings of the VII European Congress on Computational Methods in Applied Sciences and Engineering*, Crete Island, Greece.

Slika, W. and Saad, G. (2017), "A practical polynomial chaos Kalman filter implementation using non-linear error projection on a reduced polynomial chaos expansion", *Int. J. Numer. Meth. Eng.*, **112**(12), 1869-1885.

Sohn, H., Farrar, C., Hemez, F. and Czarnechi, J. (2002), "A review of Structural Health Monitoring litearture 1996-2001", (LA-UR-02-2095).

Song, J. and Der Kiureghian, A. (2006), "Generalized Bouc-Wen model for highly asymmetric hysteresis", *J. Eng. Mech.*, **132**(6), 610-618.

Spiridonakos, M.D., Chatzi, E.N. and Sudret, B. (2016), "Polynomial chaos expansion models for the monitoring of structures under operational variability", *ASCE-ASME Journal of Risk and Uncertainty in Engineering Systems, Part A: Civil Engineering*, B4016003.

St-Pierre, M. and Gingras, D. (2004), "Comparison between the unscented Kalman filter and the extended Kalman filter for the position estimation module of an integrated navigation information system", *IEEE Intelligent Vehicules Symposium*.

Welch, G. and Bishop, G. (2006), *An introduction to the Kalman Filter*, North Carolina, US, University of North Carolina: Chapel Hill.

Wiener, N. (1938), "The homogeneous chaos", *Am. J. Math.*, 897-936.

Xu, B. and He, J. (2015), "Substructural parameters and dynamic loading identification with limited observations", *Smart Struct. Syst.*, **15**(1), 169-189.

Ye, M. and Wang, X. (2007), "Parameter estimation of the Bouc-Wen hysteresis model using particle swarm optimization", *Smart Mater. Struct.*, **16**(6), 2341.

Zhang, H., Foliente, G.C., Yang, Y. and Ma, F. (2002), "Parameter identification of inelastic structures under dynamic loads", *Earthq. Eng. Struct. D.*, **31**(5), 1113-1130.

HJ